

# Log Book for *Labs into Photonics Research*

Group members: Yiming Zuo, Stijn Vandepitte, and David Okeudo

## Module 5: Fiber and Waveguide Optics

Yiming Zuo

May 28, 2025

## Contents

<b>1</b>	<b>Introduction</b>	<b>2</b>
<b>2</b>	<b>Fiber Optics</b>	<b>2</b>
2.1	Coupling Light from a 632nm Red Laser (HeNe Laser)	3
2.2	Coupling Light from an 850nm Invisible Laser	4
<b>3</b>	<b>Waveguide Optics: on-chip</b>	<b>5</b>
3.1	Grating Coupler Alignment Measurements	5
3.2	MZI measurement	7
3.3	Ring resonator	9
3.4	AWG measurement	9

# 1 Introduction

Waveguides and optical fibers are cornerstone technologies in the field of Photonics, facilitating the efficient transmission of light signals over long distances with minimal loss. These structures operate by confining light within a core of higher refractive index surrounded by a cladding of lower refractive index, utilizing the principle of total internal reflection to guide light along their paths. This capability is fundamental to modern communication systems, where long-distance, high-speed, reliable data transfer is essential.

In this laboratory session, we explored the practical and theoretical aspects of waveguides and optical fibers through a series of hands-on experiments. In the fiber optics segment, we focused on coupling light into multi-mode fibers, characterizing different fiber types by measuring their numerical apertures, and assessing fiber losses. For waveguide optics, we investigated light coupling techniques and measured propagation losses in spiral waveguides through fiber coupling in and out of grating couplers. We also characterized integrated photonic devices, including unbalanced Mach-Zehnder Interferometers (MZIs) and an Arrayed Waveguide Grating (AWG), to examine their wavelength-dependent transmission properties.

In the subsequent sections of this report, we will address the specific questions posed in the laboratory manual and present our experimental findings. These include detailed measurements of waveguide losses, characterization of integrated devices, and performance analysis of fiber-optic components. This report aims to offer a comprehensive overview of our results and their implications for advancing photonics technology.

# 2 Fiber Optics

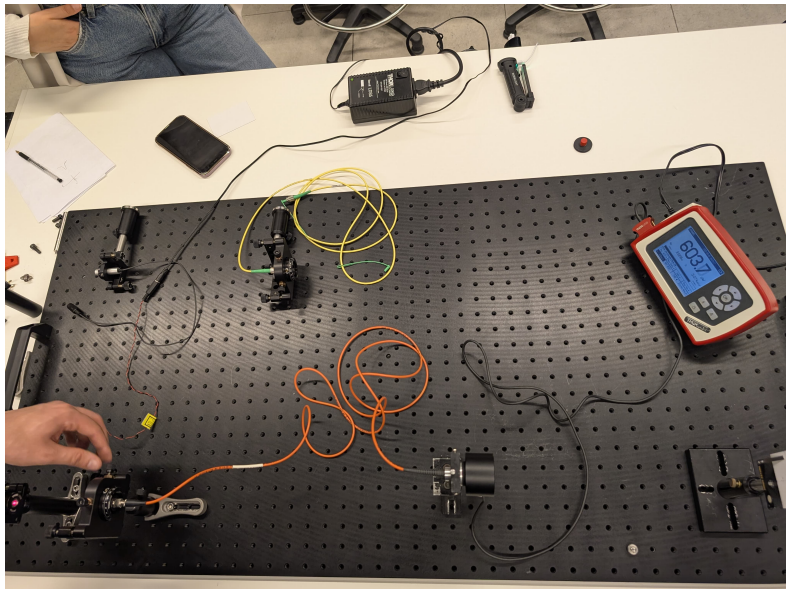


Figure 1: Fiber optics setup: lower orange fiber is multi-mode fiber being characterized first (core diameter:  $62.5\mu m$ ), upper yellow fiber is single-mode fiber being characterized later.

The morning session in the Photonics Laboratory focused on experiments involving waveguides and optical fibers, specifically coupling light into different types of fibers using both visible and invisible lasers. Below is a detailed summary of the tasks performed, based on the lab log book entries provided.

## 2.1 Coupling Light from a 632nm Red Laser (HeNe Laser)

In this session, we used a helium-neon (HeNe) laser emitting red light at 632 nm, and the light was aligned with a 2-meter-long multi-mode fiber (Figure 1). The alignment process is as follows:

- Initial raw alignment was performed by eye to position the fiber roughly in the laser beam's path;
- Fine-tuning was achieved by actively adjusting the tilt of the laser via a knob on the side to optimize the coupling efficiency. (**since the core of a multi-mode fiber has rather large cross-section(Diameter  $\approx 50 - 100\mu\text{m}$ ), the tilt of the laser turn out to be a determinant factor during alignment**)

After finishing the alignment, **power** measurement was conducted by placing a power meter at different locations:

- Input Power ( $P_{in}$ ): 1.044 mW (placed at the laser output);
- Output Power ( $P_{out}$ ): 705 uW (placed at the fiber output).

$$\text{Absorption coefficient } \alpha = -\frac{1}{L} \log \left( \frac{P_{out}}{P_{in}} \right) = -\frac{1}{0.002} \log \left( \frac{705}{1044} \right) = 196.5 \text{ km}^{-1}$$

This indicates a power loss through the fiber, likely due to coupling inefficiencies, fiber attenuation, or scattering. Additional notes to make for this section: the fiber was confirmed to be within the appropriate wavelength range for the 632 nm light and the lens used in the setup had an antireflection coating to minimize reflection losses and improve coupling efficiency.

Then we proceed to measurement of **acceptance angle**. To determine the numerical aperture of the multimode fiber, the beam diameter was measured at different distances from the fiber tip:

1. At 7.3 cm distance: Beam diameter = 4.4 cm;
2. At 4.2 cm distance: Beam diameter = 2.1 cm.

These measurements allow for the calculation of the fiber's acceptance angle, which relates to how effectively the fiber captures light.

- First, we calculate tangent of the half-angle, i.e., Ratio of radius to distance:  $x = \frac{\text{diameter}}{2 \times \text{distance}}$
- Then we can acquire numerical aperture by taking sin of the half angle,  $NA = \sin(\arctan x) = \sin \left( \arctan \left( \frac{\text{diameter}}{2 \times \text{distance}} \right) \right)$
- NA from distance 4.2 cm and diameter 2.1 cm: 0.243; NA from distance 7.3 cm and diameter 4.4 cm: 0.289; taking the average of two results from the measurement:  $NA = 0.266$ .

The NA values differ slightly (0.243 vs 0.289), possibly due to measurement error or near-field effects at 4.2 cm. The value at 7.3 cm (0.289) may be more accurate as it's farther from the fiber tip, while the average NA of approximately 0.266 provides a balanced estimate.

## 2.2 Coupling Light from an 850nm Invisible Laser

In this session, we used an invisible laser emitting at 850 nm (near-infrared range), which was coupled into a 2-meter-long single-mode fiber designed for a working wavelength of 780 nm. Since the output is invisible, we can't do the alignment by eyes, but rather completely through active alignment.

- The lens was loosened to defocus the beam to achieve a larger spot size for raw alignment, allowing a broader range for initial coupling (**since single-mode fiber's core has a rather small diameter (Diameter  $\approx 10\mu\text{m}$ )**);
- Focus the beam back and perform fine adjustments were made by tilting the source to maximize the power output.

Then we performed power measurements on this setup and results are provided below:

- Reference Power (Pin): 4.574 mW (laser output power).
- Output Power (Pout): 2.124 mW (measured at the fiber output).

The reduced output power suggests significant loss, attributed to the mismatch between the laser wavelength (850 nm) and the fiber's optimal wavelength (780 nm), causing excessive attenuation.

Finally, we did measurement on an extended fiber setup. A more complex configuration was tested by connecting: A 2-meter single-mode fiber, A connector (PC to APC, with an estimated 3% loss), A 10-km-long yellow fiber specified for the 1300–1550 nm wavelength range. The output power (Pout) turned out to be 0.780 mW. The significantly lower output power reflects losses due to the long fiber length, connector loss, and significant wavelength mismatch (850 nm is outside the 1300–1550 nm range).

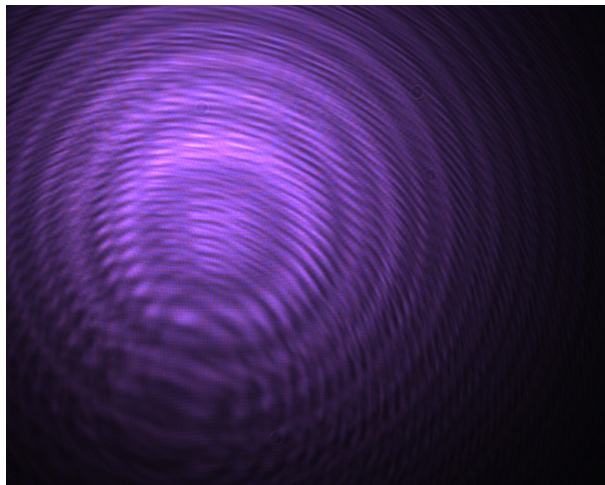


Figure 2: Fringes observed, resembling Newtonian ring

A CMOS camera was used to observe the speckle pattern of laser at the fiber output. A Newton ring-like pattern was observed, characterized by concentric rings (Figure 2). Smaller rings were hypothesized to originate from particles on the fiber surface, causing interference or scattering effects.

Key Activities and Observations  
Little summary on the tasks conducted in the morning session:

- Laser-Fiber Coupling: Experiments with a visible 632 nm HeNe laser and an invisible 850 nm laser, testing both multimode and single-mode fibers.
- Power Measurements: Quantification of input and output powers to assess coupling efficiency and fiber losses.
- Numerical Aperture Estimation: Measurement of beam diameters to characterize the acceptance angle of the multimode fiber.
- Speckle Analysis: Use of a CMOS camera to study light patterns, revealing surface-related effects.

Major loss mechanism is wavelength mismatches (e.g., 850 nm laser with a 780 nm fiber or a 1300–1550 nm fiber) led to higher losses. And apart from that, alignment precision was critical, requiring both manual and fine-tuning techniques.

### 3 Waveguide Optics: on-chip

#### 3.1 Grating Coupler Alignment Measurements

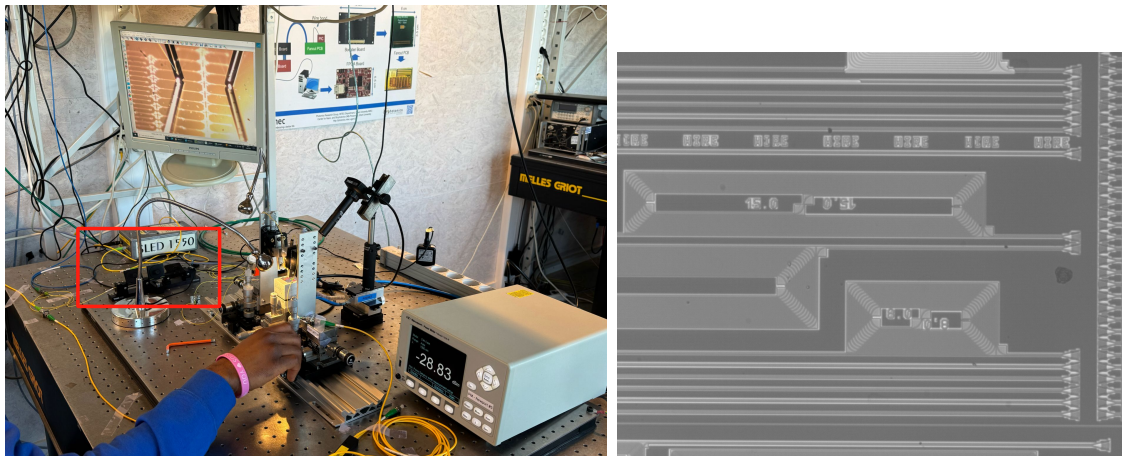


Figure 3: a) Measurement setup; b) Spiral waveguides being characterized

During the active alignment of grating couplers using a fiber controlled by mechanical arms (minimizing loss through fine tuning the position of ), several power measurements were recorded for various waveguide (wg) configurations. The input laser power, measured directly through the divider to the power meter, was -5.523 dBm (**Connector loss**). The output power levels for different configurations are summarized in the following table:

Waveguide Length (mm)	Measured Power (dBm)
8	-15.04
15	-15.80
30	-17.44
60	-19.70

Table 1: Measured power for different waveguide lengths (each with 42 waveguide bends, coupled through 2 grating couplers)

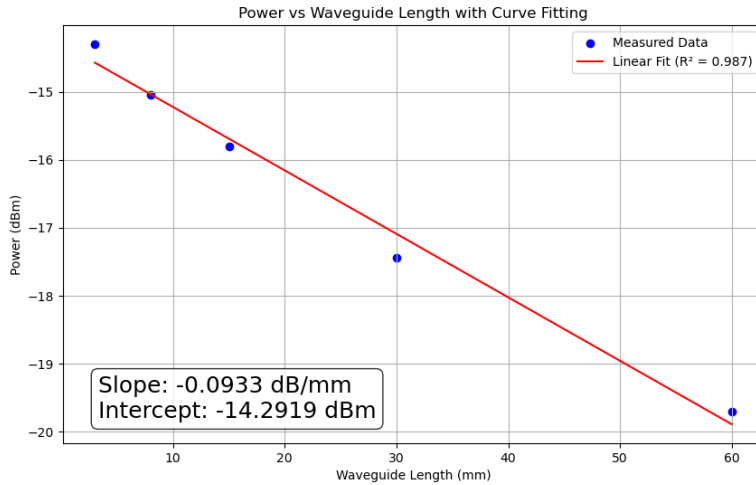


Figure 4: Linear fit of loss curve: Slope: -0.0933 dB/mm, Intercept: -14.292 dBm (bends loss + insertion loss + coupling loss by 2 grating couplers)

Input laser power is set to 1mW (0dBm). Measured power from connecting laser directly to the divider and power meter is -5.523dBm, which is the insertion loss induced by the connection of components. The output of 3mm straight waveguide (no bend) coupled through grating couplers is also measured (-14.30dBm).

A linear fit of the measured output power (in dBm) versus waveguide length (in mm) is displayed in Figure 4. The loss induced by 2 grating couplers can be extrapolated:  $14.30 - 3 * 0.0933 - 5.523 = 8.497$ dB, hence the loss of coupling into single grating coupler is half of it, 4.249 dB. This calculation aligns with the typical loss induced by grating coupler, ranging from 3-5 dB. Therefore, the loss of a single bend is  $\frac{15.04 - 8 * 0.0933 - 5.523 - 8.497}{42} = 6.51 * 10^{-3}$ dB, consistent with the preceding bend loss value,  $6.43 \times 10^{-3}$  dB per bend.

In summary, the measurements indicate a grating coupler loss of approximately 4.249 dB each, a waveguide propagation loss of about 0.09 dB/mm, and bend loss of  $6.43 \times 10^{-3}$  dB.

### 3.2 MZI measurement

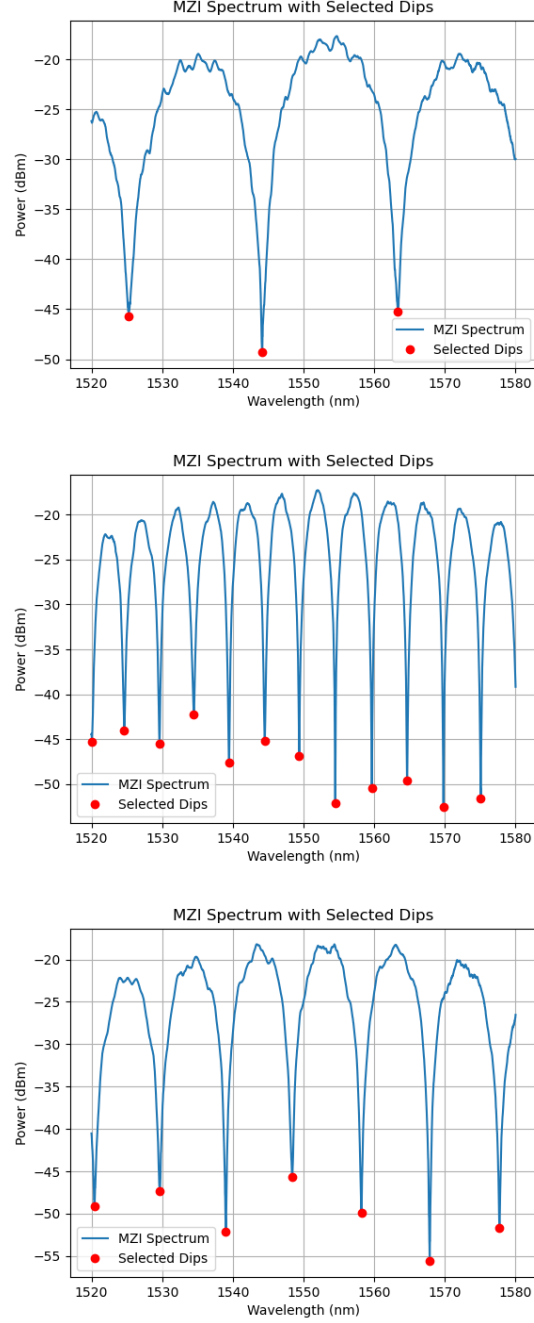


Figure 5: MZI measurement

#### Calculation of Differential Arm Length ( $\Delta L$ ):

For each pair of adjacent dip wavelengths  $\lambda_1$  and  $\lambda_2$ , the Free Spectral Range (FSR) is calculated as the difference between the two values. Assuming a group index  $n_g = 2.8$ , the differential arm length  $\Delta L$  of the MZI is computed as:

$$\Delta L = \frac{\lambda_0^2}{n_g \cdot \text{FSR}}$$

where all wavelengths are in meters. The final value of  $\Delta L$  is typically reported in micrometers ( $\mu\text{m}$ ).

### 1. MZI 1

- Selected dip wavelengths below -45 dBm (nm): 1525.30, 1544.14, 1563.32
- Free Spectral Range (FSR) and  $\Delta L$  between adjacent dips:

$\lambda_1$ (nm)	$\lambda_2$ (nm)	FSR (nm)	$\Delta L$ ( $\mu\text{m}$ )
1525.30	1544.14	18.840	44.649785
1544.14	1563.32	19.180	44.951529

Table 2: Average FSR: 19.010 nm, Average  $\Delta L$ : 44.800657  $\mu\text{m}$

### 2. MZI 2

- Selected dip wavelengths below -42 dBm (nm): 1520.08, 1524.64, 1529.62, 1534.48, 1539.46, 1544.50, 1549.40, 1554.48, 1559.66, 1564.64, 1569.80, 1575.08
- Free Spectral Range (FSR) and  $\Delta L$  between adjacent dips:

$\lambda_1$ (nm)	$\lambda_2$ (nm)	FSR (nm)	$\Delta L$ ( $\mu\text{m}$ )
1520.08	1524.64	4.560	181.514722
1524.64	1529.62	4.980	167.249429
1529.62	1534.48	4.860	172.485097
1534.48	1539.46	4.980	169.411703
1539.46	1544.50	5.040	168.487976
1544.50	1549.40	4.900	174.420868
1549.40	1554.48	5.080	169.327739
1554.48	1559.66	5.180	167.158507
1559.66	1564.64	4.980	175.008077
1564.64	1569.80	5.160	170.001282
1569.80	1575.08	5.280	167.246182

Table 3: Average FSR: 5.000 nm, Average  $\Delta L$ : 171.119235  $\mu\text{m}$

### 3. MZI 3

- Selected dip wavelengths below -45 dBm (nm): 1520.40, 1529.66, 1539.02, 1548.40, 1558.20, 1567.84, 1577.72
- Free Spectral Range (FSR) and  $\Delta L$  between adjacent dips:

$\lambda_1$ (nm)	$\lambda_2$ (nm)	FSR (nm)	$\Delta L$ ( $\mu\text{m}$ )
1520.40	1529.66	9.260	89.699032
1529.66	1539.02	9.360	89.827504
1539.02	1548.40	9.380	90.734106
1548.40	1558.20	9.800	87.927875
1558.20	1567.84	9.640	90.509467
1567.84	1577.72	9.880	89.417182

Table 4: Average FSR: 9.553 nm, Average  $\Delta L$ : 89.685861  $\mu\text{m}$

### 3.3 Ring resonator

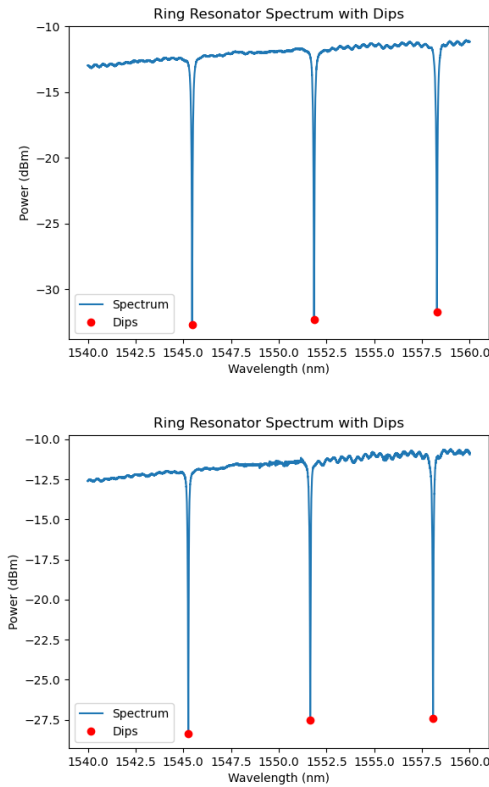


Figure 6: pass port spectra of 2 ring resonators

Table 5: Resonant Dips of Two Ring Resonators

Ring	Dip 1 (nm)	Dip 2/FSR (nm)	Dip 3/FSR (nm)
Ring 1	1545.463	1551.848	1558.284
Ring 2	1545.262	1551.648	1558.079

### 3.4 AWG measurement

Ideal: perfect phased array with focusing phase fronts ; Fabricated: phased array with distorted phase fronts. Two main contributions to phase errors: •

Waveguide-to-waveguide variations:‘long-range’ fabrication variations;temperature gradients; • Within-waveguide variations: local effective index variations (linewidth roughness)

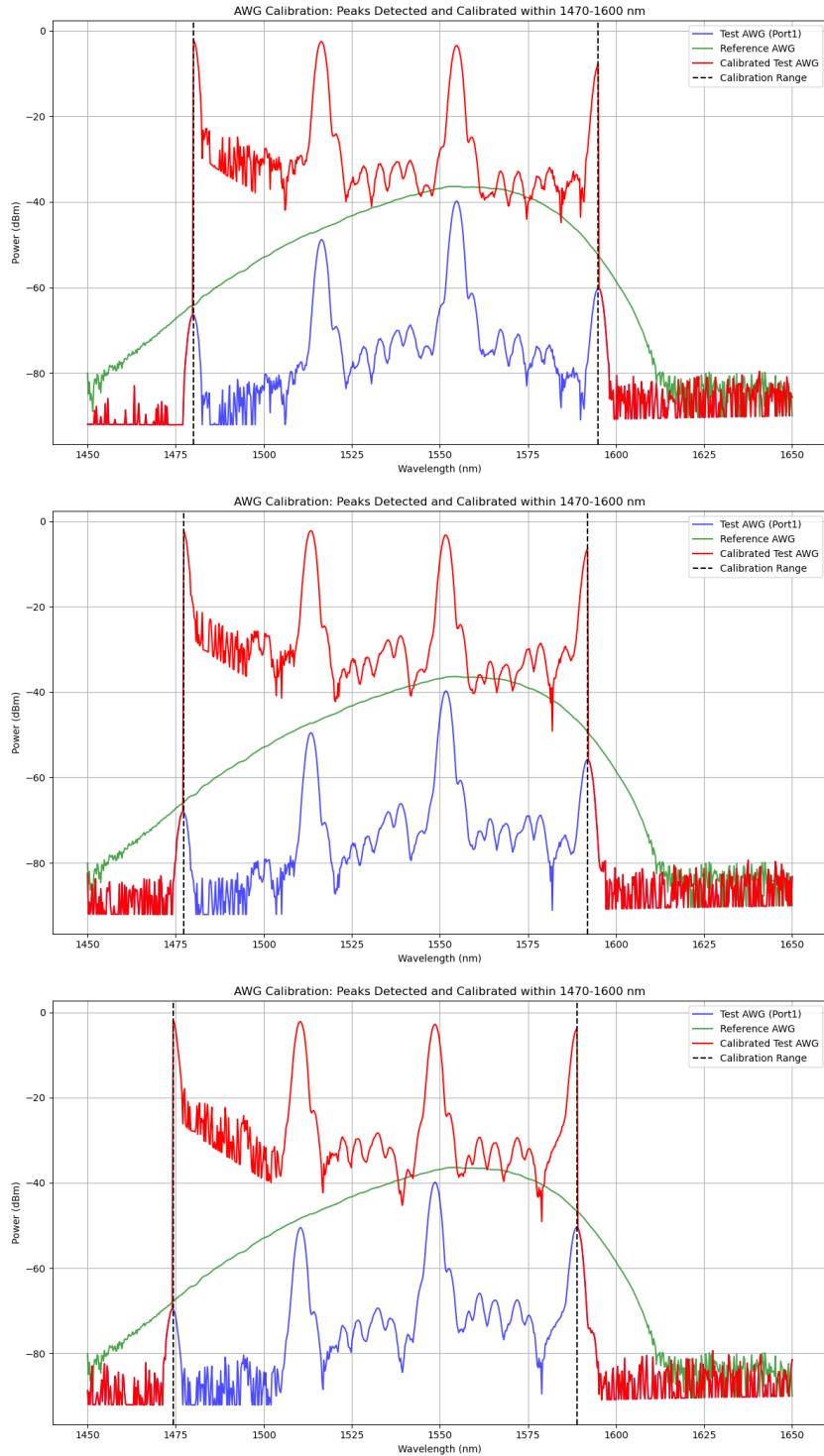


Figure 7: AWG port output spectra with corresponding detected peak wavelengths in the 1470–1600 nm range.

Table 6: Detected peak wavelengths (nm) within 1470–1600 nm

<b>AWG Port</b>	<b>Peak 1</b>	<b>Peak 2</b>	<b>Peak 3</b>	<b>Peak 4</b>
Port 1	1480.04	1516.33	1554.63	1594.93
Port 2	1477.28	1513.33	1551.63	1591.93
Port 3	1474.28	1510.33	1548.62	1588.92

The table shows peak wavelengths for three AWG ports within 1470–1600 nm: Port 1 (1480.04, 1516.33, 1554.63, 1594.93 nm), Port 2 (1477.28, 1513.33, 1551.63, 1591.93 nm), and Port 3 (1474.28, 1510.33, 1548.62, 1588.92 nm). The peaks shift by about 3 nm between ports (e.g.,  $1480.04 - 1477.28 = 2.76$  nm). This shift occurs because the AWG is designed to space channels by 3 nm, ensuring each port handles a unique wavelength. The AWG’s free spectral range (FSR) is 36 nm (e.g.,  $1516.33 - 1480.04 \approx 36.29\text{nm}$ ), so with 12 ports, the spacing per port is  $36 / 12 = 3$  nm, matching the observed shift.

Apart from that, significant side lobes are observed between the major peaks on each plot, with their wavelengths resembling those of the major peaks from adjacent ports. These side lobes originate from crosstalk between adjacent waveguides (**extremely closely spaced channels**). Since the channel waveguides between the star couplers are closely spaced, optical signals can easily couple into one another, forming significant side lobes.

A calibration of the effects of grating couplers is performed to the measured data. From the calibrated curves, loss around 4dB of each peaks can be observed. This happens because light of certain frequency component can’t be totally collected after spreading them in the free space (star coupler). So AWG is inherently lossy.